



MICROMECHANICAL APPROACH FOR FRACTURE ASSESSMENTS OF SURFACE CRACKED PLATES

Claudio Ruggieri

Department of Naval Architecture and Ocean Engineering, University of São Paulo
São Paulo, SP 05508–900, E-mail: cruggi@usp.br, Brazil

***Abstract** – This study explores the application of a micromechanics model based on the Weibull stress to predict cleavage fracture behavior in surface crack specimens loaded predominantly in tension for an A515–70 structural steel tested in the transition region. The Weibull stress parameters are calibrated using toughness data for deep notch C(T) and shallow notch SE(B) specimens. The calibrated Weibull stress model is then used to predict the toughness distribution for the surface crack specimens. The predictions of the probability distribution for cleavage fracture in the surface crack specimens based upon the present methodology agrees well with the experimental data. Such an application serves as a prototype for a wide class of engineering problems involving the transferability of fracture toughness data from laboratory specimens to structural components.*

Keywords: cleavage fracture, constraint, local approach, Weibull stress, surface crack

1. INTRODUCTION

The fundamental importance of cleavage fracture behavior in material failure has stimulated a rapidly increasing amount of research on micromechanics methodologies to assess the integrity of structural components subjected to various loading and environmental conditions. Such methodologies are collectively termed local approaches and describe the cleavage process uncoupled from the macroscopic fracture toughness (J_c , K_{Ic} or CTOD) to quantify the impact of defects in load-bearing materials and in-service structures (such as offshore and marine structures). Among these research efforts, the seminal work of Beremin provides the basis for establishing a relationship between the microregime of fracture and macroscopic crack driving forces (such as the J -integral) by introducing the Weibull stress (σ_w) as a probabilistic fracture parameter. A key feature of the Beremin approach is that σ_w follows a two-parameter Weibull distribution in terms of the Weibull modulus, m and the scale parameter, σ_u . Unstable crack propagation (cleavage) occurs at a critical value of the Weibull stress; under increased remote loading (as measured by J), differences in evolution of the Weibull stress reflects the potentially strong variations of near-tip stress fields. When implemented in a finite element code, the methodology predicts the evolution of Weibull stress with applied load (conveniently measured by J in the present work).

This study explores the application of a micromechanics model based on the Weibull stress to predict cleavage fracture behavior in surface crack specimens loaded predominantly in tension for an A515–70 structural steel tested in the transition region. The Weibull stress parameters are calibrated using toughness data for deep notch C(T) and shallow notch SE(B) specimens. The calibrated Weibull stress model is then used to predict the toughness distribution for the surface crack specimens. The predictions of the probability distribution for cleavage fracture in the surface crack specimens based upon the present methodology agrees well with the experimental data. Such an application serves as a prototype for a wide class of engineering problems involving the transferability of fracture toughness data from laboratory specimens to structural components. The proposed methodology predicts the measured statistical distribution of cleavage fracture toughness in surface crack specimens which provides a compelling support to the predictive capability of Weibull stress-based methodologies in fracture assessments of structures.

2. PROBABILISTIC MODELING OF CLEAVAGE FRACTURE

2.1 The Weibull Stress Model

Experimental studies consistently reveal large scatter in the measured values of cleavage fracture toughness for ferritic steels tested in the DBT region (see [1,2,9] for illustrative data and the experimental results presented in Section 5). A continuous probability function derived from weakest link statistics conveniently characterizes the distribution of toughness values in the form [7,16]

$$F(J_c) = 1 - \exp\left[-\left(\frac{J_c - J_{\min}}{J_0 - J_{\min}}\right)^\alpha\right], \quad (1)$$

which is a three-parameter Weibull distribution with parameters (α, J_0, J_{\min}) . Here, α denotes the Weibull modulus (*shape* parameter), J_0 defines the characteristic toughness (*scale* parameter) and J_{\min} is the *threshold* fracture toughness. Often, the threshold fracture toughness is set equal to zero so that the Weibull function given by Eq. (1) assumes its more familiar two-parameter form. The above limiting distribution remains applicable for other measures of fracture toughness, such as K_{Jc} or CTOD. A central feature emerging from this model is that, under SSY conditions, the scatter in cleavage fracture toughness data is characterized by $\alpha = 2$ for J_c -distributions or $\alpha = 4$ for K_{Jc} -distributions [3,17].

To extend the previous methodology to multiaxially stressed, 3-D crack configurations, research efforts have focused on probabilistic models which couple the micromechanical features of the fracture process (such as the inherent random nature of cleavage fracture) with the inhomogeneous character of the near-tip stress fields. Motivated by the specific micromechanism of transgranular cleavage, a number of such models (most often referred to as *local approaches*) employ weakest link arguments to describe the failure event. A central feature emerging from weakest link models is that overall fracture resistance of a macroscopic crack lying in a material containing randomly distributed flaws, as illustrated in Fig. 1, is controlled by the largest fracture-triggering particle that is sampled in the fracture process zone ahead of crack front. This region is conveniently divided in a large number of *unit* reference volumes, V_0 , statistically independent; each reference volume contains a substantially number of statistically independent microflaws uniformly distributed. Using weakest link statistics, the probability distribution for the fracture stress of a cracked solid increases with loading (represented by the J -integral) according to the two-parameter Weibull distribution [5,9,12,17]

$$\mathcal{P}(\sigma_w) = 1 - \exp\left[-\frac{1}{V_0} \int_{\Omega} \left(\frac{\sigma_1}{\sigma_u}\right)^m d\Omega\right] = 1 - \exp\left[-\left(\frac{\sigma_w}{\sigma_u}\right)^m\right], \quad \sigma_1 \geq 0, \quad (2)$$

which is a Weibull distribution with parameters m and σ_u . Here, m and σ_u denote the Weibull modulus and the scale parameter of the Weibull function, Ω represents the volume of the (near-tip) fracture process zone and σ_1 is the maximum principal stress acting on material points inside the fracture process zone. In the present work, the *active* fracture process zone is defined as the loci where $\sigma_1 \geq \lambda\sigma_0$, with $\lambda \approx 2$. Alternative definitions for the fracture process zone include the plastic region ahead of the macroscopic crack [5,6], $\sigma_e \geq \sigma_0$ where σ_e denotes the equivalent Mises stress. The stress integral appearing in Eq. (2) defines the Weibull stress, a term coined by the Beremin group [5], in the form

$$\sigma_w = \left[\frac{1}{V_0} \int_{\Omega} \sigma_1^m d\Omega\right]^{1/m}, \quad \sigma_1 \geq 0. \quad (3)$$

A central feature of this methodology involves the interpretation of σ_w as a *macroscopic* crack driving force [9-11]. Consequently, it follows that unstable crack propagation (cleavage) occurs at a critical value of the Weibull stress; under increased remote loading (as measured by J), differences in evolution of the Weibull stress reflect the potentially strong variations of near-tip stress fields.

2.2 Toughness Scaling Methodology Using Weibull Stress Trajectories

Ruggieri and Dodds [9] proposed a *toughness scaling model* based upon the Weibull stress to assess the effects of constraint variations on cleavage fracture toughness data. The central feature of this methodology

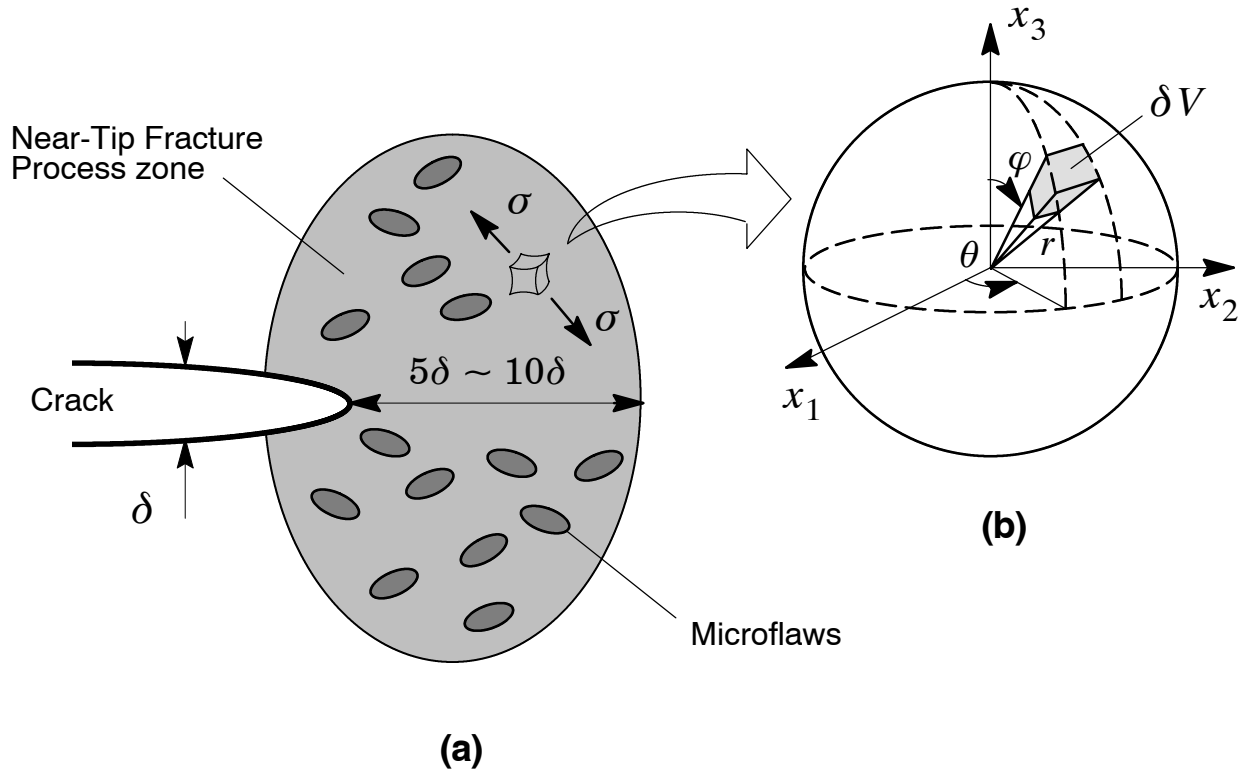


Figure 1 (a) Fracture process zone ahead a macroscopic crack containing randomly distributed flaws; (b) Unit volume ahead of crack tip subjected to a multiaxial stress state.

lies on the interpretation of σ_w as the *crack tip driving force* coupled with the simple axiom that cleavage fracture occurs when σ_w reaches a critical value, $\sigma_{w,c}$. For the same material at a fixed temperature, the scaling model requires the attainment of a specified value for σ_w to trigger cleavage fracture across different crack configurations even though the loading parameter (measured by J in the present work) may vary widely due to constraint loss. In the probabilistic context adopted here, attainment of equivalent values of Weibull stress in different cracked configurations implies the same *probability* for cleavage fracture.

Figure 2 illustrates the procedure to assess the effects of constraint loss on cleavage fracture behavior needed to scale toughness values for different cracked configurations. The procedure employs J as the measure of macroscopic loading, but remains valid for other measures of remote loading, such as K_J or CTOD. Without loss of generality, Fig. 2 displays σ_w vs. J curves for a high constrained configuration (such as a deep notch SE(B) specimen), denoted as configuration **A**, and a low constraint configuration (such as surface crack specimen under tension loading), denoted as configuration **B**. Very detailed, nonlinear 3-D finite element analyses provide the functional relationship between the Weibull stress (σ_w) and applied loading (J) for a specified value of the Weibull modulus, m . Given the J_A -value for the high constraint fracture specimen, the lines shown on Fig. 2 readily illustrate the technique used to determine the corresponding J_B -value.

3. CALIBRATION OF WEIBULL STRESS PARAMETERS

Further consideration of the toughness scaling model previously outlined led Gao et al. [13] and Ruggieri et al [14] to propose a new calibration procedure for parameter m based upon fracture toughness data measured from *two* sets of specimens. By using the Weibull stress trajectories, σ_w vs. J , for two crack configurations exhibiting different constraint levels (e.g., a deep notch and a shallow notch SE(B) specimen), the process seeks the m -value which *corrects* the corresponding measured toughness distributions. This procedure eliminates the recently discovered non-uniqueness of calibrated Weibull stress parameters [13,14] that arises when using only one set of fracture toughness data. Once determined in this manner, parameter m becomes a material property independent of specimen geometry at a fixed temperature (the test temperature).

This calibration procedure is based upon the correction of the statistical distribution for the measured toughness data based upon σ_w vs. J histories. By assuming the Weibull distribution given by Eq. (1) to describe the measured toughness data for *two* crack configurations (denoted **A** and **B**), the calibrated Weibull modulus is then defined by the m -value that *corrects* the characteristic toughness J_0^B to its equivalent J_0^A (i.e.,

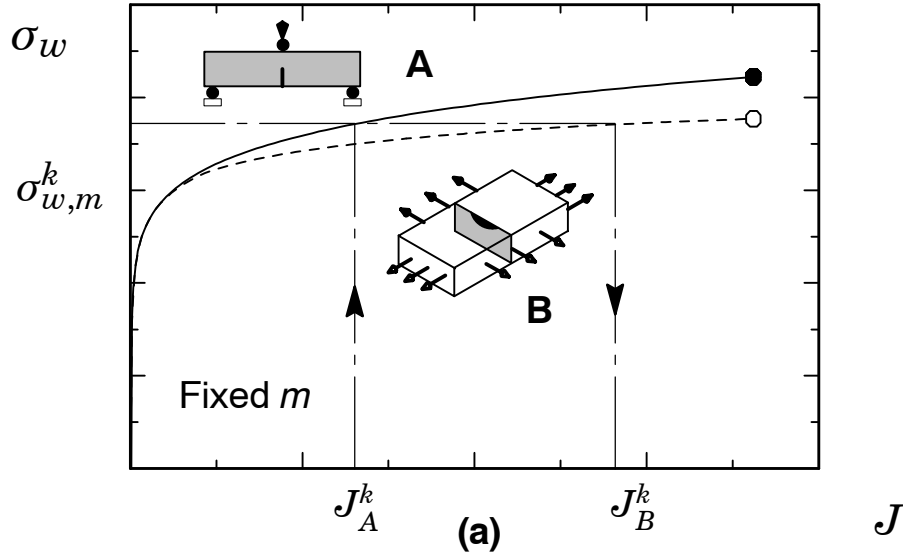


Figure 2 Toughness scaling model for different crack configurations.

$J_0^B \rightarrow J_0^A$ correction). Alternatively, the calibration can be conducted by using a two-step scheme to calibrate the m -parameter as follows: (1) constraint correct the measured toughness values for configurations **A** and **B** to corresponding plane-strain, small-scale yielding (SSY) values using the toughness scaling model based on the modified Weibull stress and (2) determine the calibrated Weibull modulus as the m -value that *corrects* the characteristic SSY toughness for configuration **B**, denoted J_{0-SSY}^B , to its equivalent characteristic SSY toughness for configuration **A**, denoted J_{0-SSY}^A . This approach retains the same scaling procedure applied on measured toughness distributions described above but corrects the two sets of fracture toughness data to have the same statistical properties under SSY conditions ($J_{0-SSY}^B \rightarrow J_{0-SSY}^A$ correction). Readers are referred to the works of Gao et al [13] and Ruggieri et al [14] for other details of parameter calibration.

4. NUMERICAL PROCEDURES AND COMPUTATIONAL MODELS

4.1. Finite Element Procedures and Constitutive Models

The three-dimensional computations reported here are generated using the research code WARP3D [18] which: (1) implements a Mises constitutive models in a finite-strain framework, (2) solves the equilibrium equations at each iteration using a linear pre-conditioned conjugate gradient (LPCG) method implemented within an element-by-element (EBE) software architecture, (3) evaluates the J -integral using a convenient domain integral procedure and (4) analyzes fracture models constructed with three-dimensional, 8-node trilinear hexahedral elements. The finite element computations employ a domain integral procedure for numerical evaluation of the J -Integral. A thickness average value for J is computed over domains defined outside material having the highly non-proportional histories of the near-tip fields and thus retains a strong domain (path) independence. Such J -values agree with estimation schemes based upon *eta*-factors for deformation plasticity. They provide a convenient parameter to characterize the average intensity of far field loading on the crack front.

The elastic-plastic constitutive model employed in the analyses follows a J_2 flow theory with conventional Mises plasticity. A piecewise linear approximation to the measured tensile response for the material is adopted to generate numerical solutions for the fracture specimens described in Section 5. The uniaxial stress-strain curve for the A515-70 pressure vessel steel at the test temperature, $T = 266$ K (-7°C) and $T = 245$ K (-28°C) is described in [15]. The material has a Young's modulus $E = 200$ GPa, Poisson's ration $\nu = 0.3$ and yield stress $\sigma_0 = 280$ MPa at 266 K (-7°C) and $\sigma_0 = 300$ MPa at 245 K (-28°C). Readers are also referred to the works of Ruggieri et al [21] for further details.

4.2. Finite Element Models

3-D finite element analyses are conducted on different crack configurations which include: (1) a conventional, plane sided C(T) specimen with $a/W = 0.6$, $B = 25$ mm and $W = 50$ mm; (2) a conventional, plane sided

SE(B) specimen with $a/W=0.2$, $B=25$ mm, $W=50$ mm and $S=4W$ and (3) a bolt-loaded surface crack SC(T) specimen with $a/t=0.25$, $c/a=3$ and $t=25$ mm. For the C(T) and SE(B) specimens, a is the crack length, W is the specimen width, B is the specimen thickness and S is the bend specimen span. For the SC(T) specimen, a is the maximum depth of the surface crack, $2c$ is the length of the semi-elliptical crack and t is the thickness of the cracked section.

Figure 3 (a) shows the geometry and specimen dimensions of the bolt-loaded SC(T) specimen [15,19]. Figure 3 (b) displays the finite element model constructed for the 3-D analyses of this specimen. Symmetry conditions enable analyses using one-quarter of the 3-D model with appropriate constraints imposed on the symmetry planes. A focused ring of elements surrounding the crack front in the radial direction is used with a small key-hole at the crack tip; the radius of the key-hole, ρ_0 , is $2.5\mu\text{m}$. The half-length of the semi-elliptical crack is defined by 20 elements arranged over the (one-half) crack front. The quarter-symmetric, 3-D model for the SC(T) specimens has 25650 nodes and 22800 elements. The models for the C(T) and SE(B) specimens have similar features and similar levels of mesh refinement. These meshes have 10 variable thickness layers defined over the half-thickness ($B/2$); the thickest layer is defined at $Z=0$ with thinner layers defined near the free surface ($Z=B/2$) to accommodate strong Z variations in the stress distribution. The quarter-symmetric, 3-D models for the C(T) and SE(B) specimens have 11800 nodes and 9800 elements.

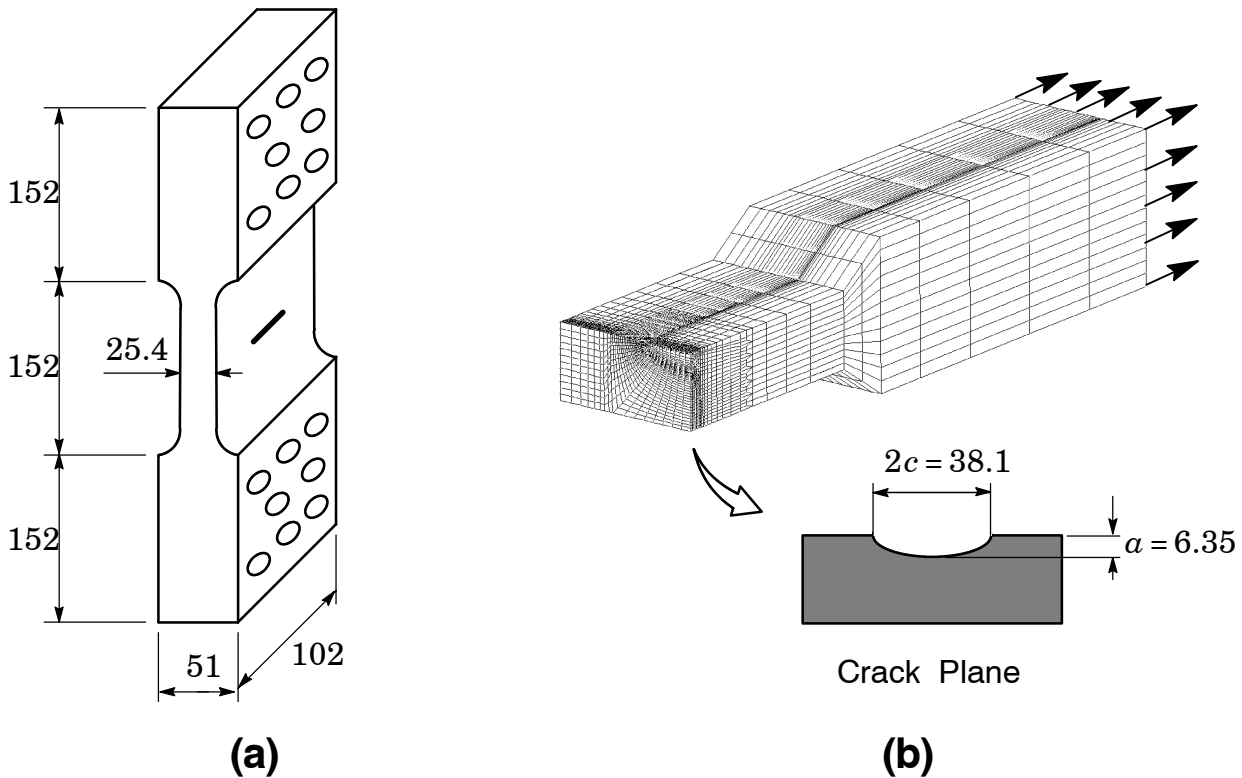


Figure 3 (a) Geometry of bolt-loaded surface crack specimen; (b) Quarter-symmetric finite element model for bolt-loaded surface crack specimen.

4.3 Finite Element Form of the Weibull Stress

Numerical computations of the Weibull stress used to construct σ_w vs. J trajectories are performed using the research code WSTRESS [12] which implements a finite element form of Beremin's formulation [5]. In isoparametric space, the current (deformed) Cartesian coordinates x_i of any point inside a 8-node tri-linear element are related to the parametric coordinates η_i using the shape functions corresponding to the k -th node. Let \mathcal{J} denote the determinant of the standard coordinate Jacobian between deformed Cartesian and parametric coordinates. Then using standard procedures for integration over element volumes, the Weibull stress has the form

$$\sigma_w = \left[\frac{1}{V_0} \sum_{n_e} \int_{\Omega_e} (\sigma_1)^m d\Omega_e \right]^{1/m} = \left[\frac{1}{V_0} \sum_{n_e} \int_{-1}^1 \int_{-1}^1 \int_{-1}^1 (\sigma_1)^m d\eta_1 d\eta_2 d\eta_3 \right]^{1/m} \quad (4)$$

where n_e is the number of elements inside the fracture process zone near the crack tip and Ω_e is the volume of the element. The process zone used here includes all material inside the loci $\sigma_1 \geq \lambda\sigma_0$, with $\lambda = 2$; results for σ_w differ little over a wide range of λ -values. For computational simplicity, an element is included in the fracture process zone if the σ_1 computed at $\eta_1 = \eta_2 = \eta_3 = 0$ (*i.e.*, the center of element) exceeds $2\sigma_0$.

5. CLEAVAGE FRACTURE PREDICTIONS FOR FRACTURE SPECIMENS

5.1. Experimental Toughness Data

Gao et al [15] recently reported a series of fracture toughness tests conducted by Joyce and Link [19] and Tregoning [20] on a C-Mn alloy pressure vessel steel. The fracture mechanics tests include: (1) a conventional, plane sided C(T) specimen with $a/W = 0.6$, $B = 25$ mm and $W = 50$ mm; (2) a conventional, plane sided SE(B) specimen with $a/W = 0.2$, $B = 25$ mm, $W = 50$ mm and $S = 4W$ and (3) a bolt-loaded surface crack SC(T) specimen with $a/t = 0.25$, $c/a = 3$ and $t = 25$ mm (see Section 4.3). The material is an A515-70 pressure vessel steel (280 MPa yield stress at 266 K (-7°C)) with relatively high hardening properties ($\sigma_u/\sigma_{ys} \approx 2$).

Testing of these configurations was performed at $T = 245$ K (-28°C) for the C(T) specimens and $T = 266$ K (-7°C) for the SE(B) and SC(T) specimens; these temperatures correspond to the ductile-to-brittle transition behavior for the material. Figure 4(a) provides a Weibull diagram of the measured toughness values for both test temperatures. The solid symbols in the plots indicate the experimental fracture toughness data for the specimens. Values of cumulative probability, F , are obtained by ordering the J_c -values and using $F = (i-0.3)/(N+0.4)$, where i denotes the rank number and N defines the total number of experimental toughness values. The straight lines indicate the three-parameter Weibull distribution, Eq. (1), obtained by a maximum likelihood analysis of the data set with $J_{\min} = 1.8$ KJ/m² ($K_{J-\min} = 20$ MPa $\sqrt{\text{m}}$). While the Weibull slopes for the C(T) and SE(B) toughness distributions are very similar ($\alpha \approx 2$ for both distributions), the results clearly demonstrate a strong effect of constraint level on the characteristic toughness, J_0 (the J -value corresponding to 63.2% failure probability). In contrast, the Weibull slope for the SC(T) specimen differ significantly ($\alpha \approx 10$) from the α -value for the C(T) and SE(B) specimens; here, the SC(T) and SE(B) specimen have similar values for the characteristic toughness, J_0 . The large deviation of the Weibull slope for the SC(T) specimen from the SSY value $\alpha = 2$ is most likely associated with the strong tensile field that develops ahead of crack front for this specimen. The tested bolt-loaded crack configuration has a symmetrical geometry (see Fig. 3) which provides a predominantly tensile loading with only small bending moments acting on the crack plane [15]. Consequently, the near-tip stresses relax significantly from the SSY levels with rapid development of plasticity in the crack ligament thereby decreasing the amount of scatter in toughness values (*i.e.*, increasing the Weibull modulus, α). Readers are referred to Joyce and Link [19] and Gao et al. [15] for a more complete presentation of testing details.

5.2. Calibration of Weibull Stress Parameters

The parameter calibration scheme described in Section 3 is applied to determine the Weibull stress parameters for the tested pressure vessel steel. The Weibull modulus, m , is calibrated using the deep notch C(T) specimens and the shallow notch SE(B) specimens. Because the specimens were not tested at the same temperature, the present methodology adopts a simple procedure to correct the measured toughness values for temperature. The J_0 -value for the C(T) specimens at 245 K (-28°C) is *scaled* to corresponding J_0 -value at 266 K (-7°C) using the Master Curve fitting given by ASTM E-1921 [4]. Since the toughness values for this specimen are below the limit value $K_{Jc} = \sqrt{Eb_0\sigma_0/M}$ with the deformation limit $M = 30$ given by ASTM E-1921, they are taken directly as SSY toughness values at 245 K (-28°C). The potential effects of (small) constraint loss on the C(T) specimens (with implications on T_0) are considered to have minor impact on the calibrated m -value. Moreover, this procedure enables determination of the reference temperature, T_0 , and the J_c -distribution at 266 K (-7°C) in a straightforward manner. The characteristic toughness values for the C(T) and SE(B) specimens at 266 K (-7°C) are then given as: $J_0^{\text{C(T)}} \approx 54$ KJ/m² and $J_0^{\text{SE(B)}} \approx 102$ KJ/m².

With the toughness values for the C(T) and SE(B) specimens set at the same temperature of 266 K (-7°C) and using σ_w vs. J curves constructed from the 3-D finite element analyses for both crack configurations, the

calibration procedure is then applied to determine the m -value that yields the same σ_w for the pair $(J_0^{C(T)}, J_0^{SE(B)})$. For the tested material, the analysis provides the Weibull stress modulus as $m \approx 8$.

5.3. Fracture Predictions Using The Weibull Stress Model

To verify the predictive capability of the Weibull stress methodology adopted in the present work, this section describes application of the toughness scaling model based on the Weibull stress (σ_w) to predict the toughness distribution for the bolt-loaded surface crack specimen. Very detailed 3-D, nonlinear finite element analyses provide crack front stress fields to generate the evolution of σ_w vs. J for the m -values calibrated in the previous section.

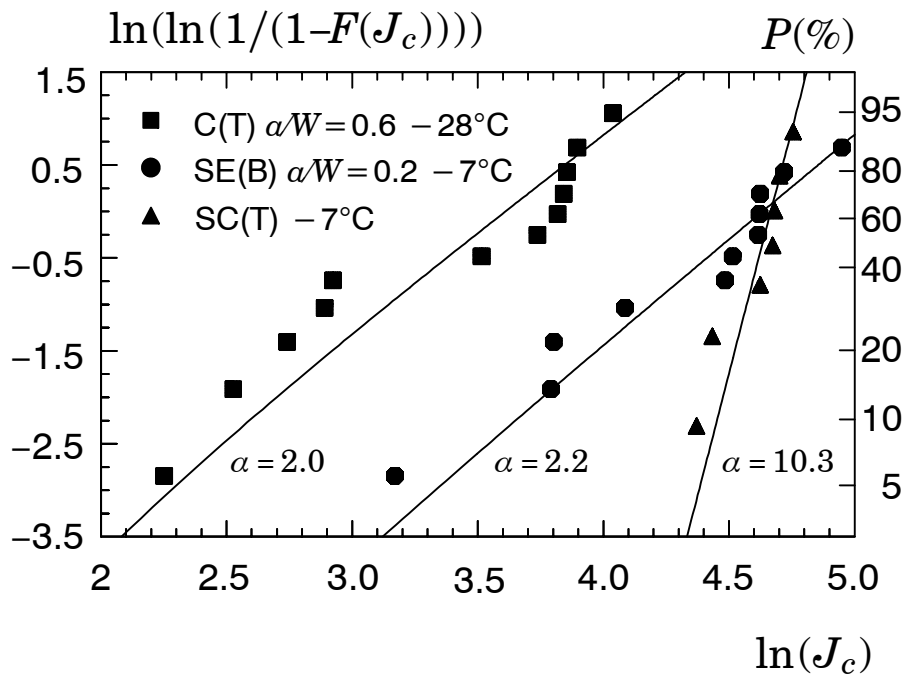
The Weibull probability plot in Fig. 4(b) shows the predicted distributions of cleavage fracture toughness for the bolt-loaded surface crack specimen using the calibrated micromechanics model. The solid symbols in the plots indicate the measured cleavage fracture toughness (J_c) for this specimen. Values of cumulative probability, F , are obtained by ordering the J_c -values and using $F = (i-0.3)/(N+0.4)$, where i denotes the rank number and N defines the total number of experimental toughness values. The solid line on each figure represents the *predicted* Weibull distribution generated from the *distribution* (not individual values from tested specimens) of toughness values for the C(T) specimen with $a/W = 0.6$ using a statistical procedure based upon Monte Carlo simulation. The dashed lines represent the 90% confidence bounds generated from the 90% confidence limits for the calibrated m -values using the scheme proposed by Ruggieri [21].

The ability of the present model in describing general fracture behavior for this specimen is evident as the predicted distribution displayed in Fig. 4(b) agrees relatively well with the experimental data. Here, the 90% confidence bounds bracket most of the measured toughness values in the mid-region of the curves. The results also indicate that the predicted curves: (1) overpredict the failure probability in the lower tail of the plots and (2) underpredict the failure probability in the upper tail of the plots. However, such deviations from the experimentally measured distribution should not be pessimistically interpreted as the small number of J_c -values available ($N = 7$) contributes to penalize a better agreement between the predictions and experiments. Perhaps more importantly, the toughness distribution for the bolt-loaded SC(T) specimen differs significantly from the toughness distribution for the shallow notch SE(B) specimen even though both specimens have similar levels of characteristic toughness (recall the Weibull slopes for the toughness distributions of these specimens displayed on Fig. 4(b) are very different); such feature most likely imposes an additional penalty on the prediction process.

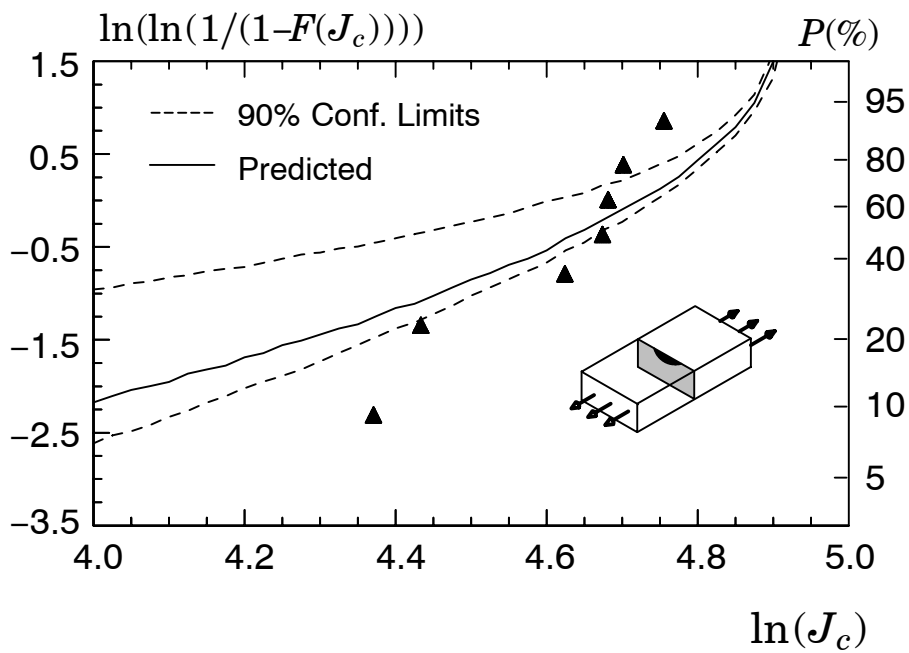
6. DISCUSSIONS AND CONCLUDING REMARKS

This study describes a probabilistic framework based on the Weibull stress (σ_w) model to predict the effects of constraint loss on macroscopic measures of cleavage fracture toughness (K_{Ic} , J_c , δ_c) applicable for ferritic materials in the ductile-to-brittle transition region. The central feature of this methodology lies on the interpretation of σ_w as the *crack tip driving force* coupled with the simple axiom that cleavage fracture occurs when the Weibull stress reaches a critical value, $\sigma_{w,c}$. For the same material at a fixed temperature, the scaling model requires the attainment of a specified value for σ_w to trigger cleavage fracture across different crack configurations even though the loading parameter (measured by J in the present work) may vary widely due to constraint loss.

The predictions of the probability distribution for cleavage fracture in a surface crack specimen based upon the present methodology agrees well with the experimental data. While the failure probabilities for lower toughness values (the lower tail of the curves) are somewhat overpredicted, the Weibull stress models appear to capture general fracture behavior for the SC(T) specimen. While the present study has not explored other ranges of crack configurations, loading modes and, most importantly, other material properties to verify the real significance of three-parameter Weibull stress models in fracture behavior predictions, the results presented here represent a compelling support to the predictive capability of Weibull stress-based methodologies.



(a)



(b)

Figure 4 (a) Weibull plots of experimental toughness values at $T=245\text{ K}$ (-28°C) and 266 K (-7°C) [15]; (b) Cleavage fracture predictions for the SC(T) specimen using the C(T) specimens.

Acknowledgements

This investigation was supported by grants principally from the Scientific Foundation of the State of São Paulo (FAPESP) under Grant 98/10574-2 and 01/06919-9. The author is indebted to Prof. Robert H. Dodds (University of Illinois) for many valuable discussions and for making available the finite element model for the SC(T) specimens.

REFERENCES

1. Sorem, W.A., Dodds, R.H., and Rolfe, S.T., "Effects of Crack Depth on Elastic Plastic Fracture Toughness," *International Journal of Fracture*, Vol. 47, pp. 105–126, 1991.
2. Wiesner, C. S. and Goldthorpe, M. R., "The Effect of Temperature and Specimen Geometry on the Parameters of the Local Approach to Cleavage Fracture" in *International Conference on Local Approach to Fracture (MECAMAT 96)*, Fontainebleau, France, 1996, pp. C6-295–304.
3. Wallin, K. "The Scatter in K_{Ic} Results," *Engineering Fracture Mechanics*, Vol. 19, pp. 1085–1093, 1984.
4. American Society for Testing and Materials, "Test Methods for the Determination of Reference Temperature, T_0 , for Ferritic Steels in the Transition Region," ASTM E-1921, Philadelphia, 1998.
5. Beremin, F.M., "A Local Criterion for Cleavage Fracture of a Nuclear Pressure Vessel Steel," *Metallurgical Transactions*, Vol. 14A, pp. 2277–2287, 1983.
6. Mudry, F., "A Local Approach to Cleavage Fracture", *Nuclear Engineering and Design*, Vol. 105, pp. 65–76, 1987.
7. Weibull, W., "The Phenomenon of Rupture in Solids", *Ingeniors Vetenskaps Akademien, Handlingar*, Vol. 153, pp. 55, 1939.
8. Ruggieri, C., "Probabilistic Treatment of Brittle Fracture Using Two Failure Models," *Probabilistic Engineering Mechanics*, Vol. 13, pp. 309–319, 1998.
9. Ruggieri, C. and Dodds, R. H., "A Transferability Model for Brittle Fracture Including Constraint and Ductile Tearing Effects: A Probabilistic Approach," *International Journal of Fracture*, Vol. 79, pp. 309-340, 1996.
10. Ruggieri, C. and Dodds, R. H., "Probabilistic Modeling of Brittle Fracture Including 3-D Effects on Constraint Loss and Ductile Tearing," *Journal de Physique*, Vol. 1996.
11. Ruggieri, C., Dodds, R. H. and Wallin, K., "Constraints Effects on Reference Temperature, T_0 , for Ferritic Steels in the Transition Region," *Engineering Fracture Mechanics*, Vol. 60, pp. 19-36, 1998.
12. Ruggieri, C. and Dodds, R. H., "WSTRESS Release 2.0: Numerical Computation of Probabilistic Fracture Parameters for 3-D Cracked Solids," *BT-PNV-51 (Technical Report)*, EPUSP, University of São Paulo, 2001.
13. Gao, X., Ruggieri, C. and Dodds, R. H., "Calibration of Weibull Stress Parameters Using Fracture Toughness Data". *International Journal of Fracture*, Vol. 92, pp. 175–200, 1998.
14. Ruggieri, C., Gao, X. and Dodds, R. H., "Transferability of Elastic–Plastic Fracture Toughness Using the Weibull Stress Approach: Significance of Parameter Calibration". *Engineering Fracture Mechanics*, Vol. 67, pp. 101–117, 2000.
15. Gao, X., Dodds, R. H., Tregoning, R. L., Joyce, J. A. and Link, R. E., "A Weibull Stress Model to Predict Cleavage Fracture in Plates Containing Surface Cracks". *Fatigue and Fracture of Engineering Materials and Structures*, Vol. 22, pp. 481–493, 1999.
16. Mann, N. R., Schafer, R. E. and Singpurwalla, N. D., *Methods for Statistical Analysis of Reliability and Life Data*, John Wiley & Sons, New York, 1974.
17. Minami, F., Brückner-Foit, A., Munz, D. and Trollenier, B., "Estimation Procedure for the Weibull Parameters Used in the Local Approach," *International Journal of Fracture*, Vol. 54, pp. 197–210, 1992.
18. Koppenhoefer, K., Gullerud, A., Ruggieri, C., Dodds, R. and Healy, B., "WARP3D: Dynamic Nonlinear Analysis of Solids Using a Preconditioned Conjugate Gradient Software Architecture", *Structural Research Series (SRS) 596*, UILU-ENG-94-2017, University of Illinois at Urbana-Champaign, 1994.
19. Joyce, J. A. and Link, R. E., "Ductile-to-Brittle Transition Characterization Using Surface Crack Specimens Loaded in Combined Tension and Bending," in *Fatigue and Fracture Mechanics: 28th Volume, ASTM STP 1321*, J. H. Underwood, et al. Eds., American Society for Testing and Materials, Philadelphia, pp. 243–262, 1997.
20. Tregoning, R., Unpublished Experimental Data, 1998.
21. Ruggieri, C., "Influence of Threshold Parameters on Cleavage Fracture Predictions Using the Weibull Stress Model". *International Journal of Fracture*, Vol. 110, pp. 281–304, 2001.